

PAPER • OPEN ACCESS

A levitated atom-nanosphere hybrid quantum system

To cite this article: A Hopper and P F Barker 2024 *New J. Phys.* **26** 013015

View the [article online](#) for updates and enhancements.

You may also like

- [Characterisation of a charged particle levitated nano-oscillator](#)
N P Bullier, A Pontin and P F Barker
- [Levitated electromechanics: all-electrical cooling of charged nano- and micro-particles](#)
Daniel Goldwater, Benjamin A Stickler, Lukas Martinetz et al.
- [Searching for new physics using optically levitated sensors](#)
David C Moore and Andrew A Geraci



PAPER

A levitated atom-nanosphere hybrid quantum system

OPEN ACCESS

RECEIVED

15 September 2023

REVISED

6 December 2023

ACCEPTED FOR PUBLICATION

2 January 2024

PUBLISHED

10 January 2024

Original Content from
this work may be used
under the terms of the
[Creative Commons
Attribution 4.0 licence](#).

Any further distribution
of this work must
maintain attribution to
the author(s) and the title
of the work, journal
citation and DOI.

A Hopper and P F Barker* 

Department of Physics and Astronomy, University College London, London, United Kingdom

* Author to whom any correspondence should be addressed.

E-mail: p.barker@ucl.ac.uk**Keywords:** levitated optomechanics, cold atoms, hybrid quantum systems, cold atom collisions**Abstract**

Near-field, radially symmetric optical potentials supported by a levitated nanosphere can be used for sympathetic cooling and for creating a bound nanosphere-atom system analogous to a large molecule. We demonstrate that the long range, Coulomb-like potential produced by a single blue detuned field increases the collisional cross-section by eight orders of magnitude, allowing fast sympathetic cooling of a trapped nanosphere to microKelvin temperatures using cold atoms. By using two optical fields to create a combination of repulsive and attractive potentials, we demonstrate that a cold atom can be bound to a nanosphere creating a new levitated hybrid quantum system suitable for exploring quantum mechanics with massive particles.

1. Introduction

The ability to cool and manipulate the centre-of-mass motion of isolated nanoparticles levitated in vacuum is seen as an important enabling technology for exploring macroscopic quantum mechanics at mass scales well beyond the current state-of-the-art (25×10^3 amu) [1]. Experiments have been proposed for studying wavefunction collapse, entanglement, decoherence, and for probing the quantum nature of gravity of particles in the $10^6 - 10^{10}$ amu mass range [2–6]. As a levitated particle in vacuum is much like a large atomic or molecular system, it can be cooled and trapped using techniques first developed in atomic physics [7, 8]. Over the last ten years, significant progress has been made towards cooling both the centre-of-mass motion and the also the internal temperature of levitated nanoparticles [9–11]. Cavity cooling and feedback cooling to near the motional ground state has very recently been demonstrated, with temperatures reaching the 10 μ K range, bringing these systems well into the quantum regime [12, 13].

Sympathetic cooling of the centre-of-mass motion by elastic collisions with a cold gas is another route towards creating cold trapped nanoparticles [14]. These methods have been very successful in creating both ultra-cold atoms and molecules that cannot be laser-cooled [15], with temperatures recently reaching 200 nK. Sympathetic cooling via the coupling of the thermal motion of cold atoms to a levitated nanosphere with a mediating cavity light field has also been proposed [16] while more recently sympathetic cooling of YIG nanosphere via an ultra-cold spin-polarized gas has been proposed [14]. Lastly sympathetic cooling mediated by the Coulomb interaction between co-trapped nanospheres in Paul traps and magnetic [17–19] and by optical binding have been realized [20]. Temperatures so far are currently limited to the mK range.

Unlike other quantum optomechanical systems, cold levitated nanoparticles can also be released from the trap, allowing matter-wave interferometry and the measurement of small forces, in the absence of perturbing trapping fields. However, unlike an atomic system, most levitated nanoparticles do not typically have well-defined internal quantum states that can be coherently manipulated and used for interferometry. A type of Ramsey interferometry using a single nanoscale particle has been proposed. This uses the spin of a single nitrogen vacancy ($S = 1$, $N-V^{-1}$) as a well-controlled quantum system that is embedded within a levitated nanodiamond [21]. However, while this general scheme is a promising way to evidence non-classicality in the centre-of-mass motion of a massive quantum system, in optical traps it has so far been plagued by technical issues due in large part to the high internal temperature inherent in these levitation schemes as well as rotation of the crystal while trapped [22, 23]. High temperatures lead to phonon broadening of the internal states as well as both motional and spin decoherence, while rotational/librational motion can

hamper the use of this system for matter-wave interferometry, [24, 25]. Despite these problems, it has recently been used to demonstrate spin cooling [26]. Recently, a hybrid nanosphere-atom system has been proposed [27] as a method to create centre-of-mass quantum superpositions using an atom associated with the nanoparticle via a scattered optical field.

In this paper, we describe a different type of levitated hybrid quantum system, which utilises the good control over both the internal and external degrees of freedom of cold atoms when trapped within optical potentials centred around a nanosphere. The optical potentials are created by both incident and scattered light fields and can be tuned by controlling laser intensity and wavelength. Here the atom can be bound closely to the nanosphere creating a well defined quantum system akin to a molecule with quantised vibrational motion. This system is attractive because atoms can be strongly bound to the nanosphere via the optical fields, but, unlike an NV nanodiamond or quantum dot where the quantum emitter is embedded in the macroscopic object, they are well isolated from the surface and are therefore not subject to phonon broadening or lattice effects. Finally, we show that these optical potentials can be used to increase the collisional cross-section of the nanoparticle enabling rapid thermalization via collisions with cold atoms offer a new general scheme for cooling levitated nanoparticles.

2. Radially symmetric optical potentials

We consider a dielectric nanosphere that is levitated in a Paul trap in high vacuum [28]. To create a radially symmetric optical potential around the nanosphere it is illuminated with three weakly focused optical fields propagating in orthogonal directions, as shown in figure 1. When the particle is significantly smaller than the wavelength of light, the scattered electric field and intensity can be readily calculated in the Rayleigh approximation [29]. For a polarizable particle illuminated by an incident optical field $E = E_0 \exp i(kx - \omega t)$, propagating in the x direction and polarized along the z direction, the total field due to both the incident and scattered field in the radial and azimuthal directions using spherical polar co-ordinates is given by

$$\begin{aligned} E_r &= CE \cos \theta \left[\frac{2}{k^2 r^2} - \frac{2i}{kr} \right] \frac{k^2}{r} + E \cos \theta + c.c. \\ E_\theta &= CE \sin \theta \left[\frac{1}{k^2 r^2} - \frac{i}{kr} - 1 \right] \frac{k^2}{r} - E \sin \theta + c.c. \end{aligned} \quad (1)$$

For this polarization there is no ϕ dependence in the field, and $C = \alpha/4\pi\epsilon_0 = a^3(n^2 - 1)/(n^2 + 2)$ where α is the polarizability of the nanosphere, a is the radius of the nanoparticle of refractive index n , $k = 2\pi/\lambda$ is the wavevector of the light, and λ is its wavelength. The total near-field irradiance or intensity around the nanosphere from a single plane wave is then given by

$$I_s = I_0 \frac{[4Cr^3 + r^6 + 4C^2(1 + k^2r^2)]}{r^6} \cos^2 \theta + I_0 \frac{[r^6 - 2Cr^3(1 - k^2r^2) + C^2(1 - k^2r^2 + k^4r^4)]}{r^6} \sin^2 \theta \quad (2)$$

where $I_0 = 1/2\epsilon_0 c E_0^2$. Figure 2(a) shows a plot of the near field intensity around the nanoparticle, with radius $a = 40$ nm, refractive index $n = 1.43$ and wavelength 1000 nm. Note that in contrast to the far-field scattered radiation, the near field scattered intensity is maximized along the polarization direction. As this simple analytical solution only applies in the Rayleigh regime when $a \ll \lambda$, we confirm that this is a good approximation for this radius by performing numerical simulations by finite difference time domain calculations using the Lumerical software package [30]. In order to create a spherically symmetric optical near-field potential, we illuminate the particle with three fields, with orthogonal angles of incidence and polarization. When the three optical fields with angles θ of $\cos^{-1}(x/r)$, $\cos^{-1}(y/r)$, $\cos^{-1}(z/r)$ are added incoherently, the total intensity is given by

$$I_T = I_0 \left[3 + \frac{6C^2}{r^6} + \frac{2C^2k^2}{r^4} + \frac{2C^2k^4}{r^2} + \frac{4Ck^2}{r} \right]. \quad (3)$$

We choose the wavevectors of the three incident fields such that $k \approx k_1 \approx k_2 \approx k_3$. A plot of this combined intensity in the y - x plane is shown in figure 2(b), which illustrates the radial spherical symmetry around the nanosphere. Note that the radial dependence of the total field is dependent on the wavelength of light through the wavevector $k = \frac{2\pi}{\lambda}$, which is dominated at short range by the $1/r^6$ term, and by the $1/r$ term at long range.

The interaction of the optical field with either the atom or the nanosphere induces an oscillating dipole moment that leads to an optical dipole potential given by $U_{\text{dip}}(r) = -\frac{1}{2} \frac{\alpha I(r)}{\epsilon_0 c}$, where α is the polarizability of

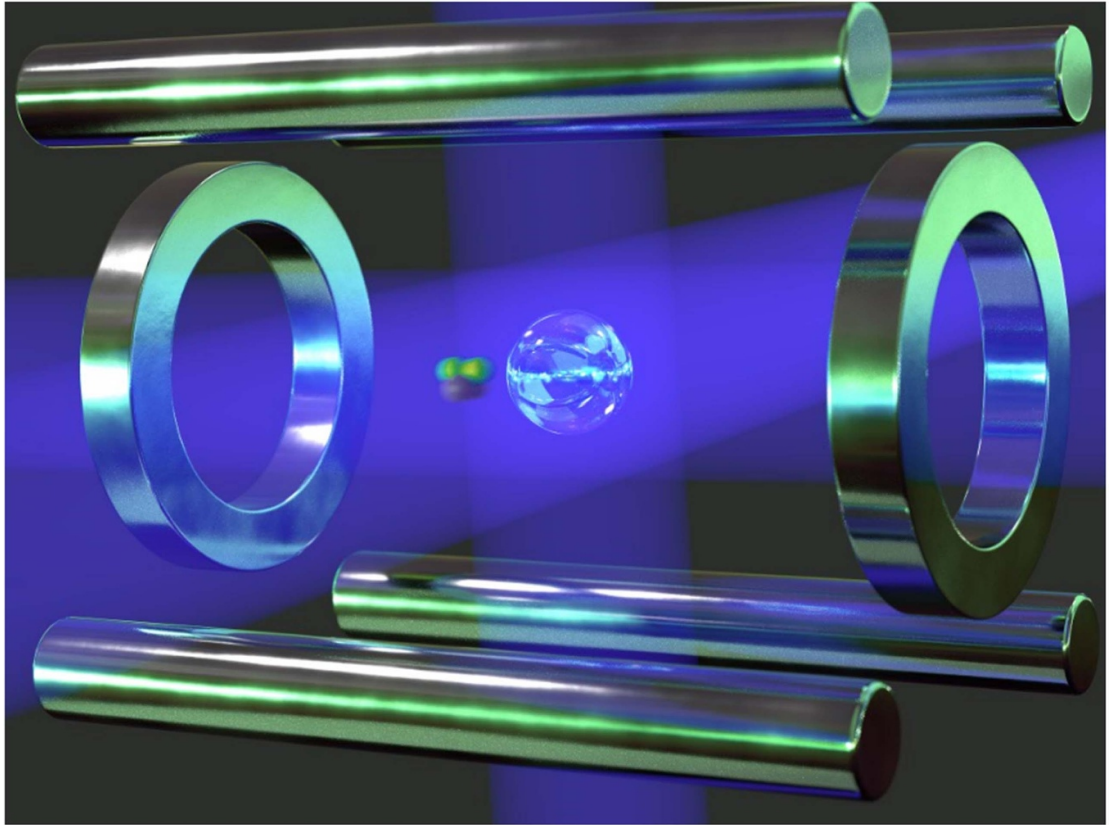


Figure 1. A diagram illustrating the creation of a spherically symmetric radial optical potential around a nanosphere trapped in a Paul trap. The potential, which is always centred on the nanosphere, is created by both the incident and scattered fields from three loosely focused orthogonally polarized optical fields, shown in blue.

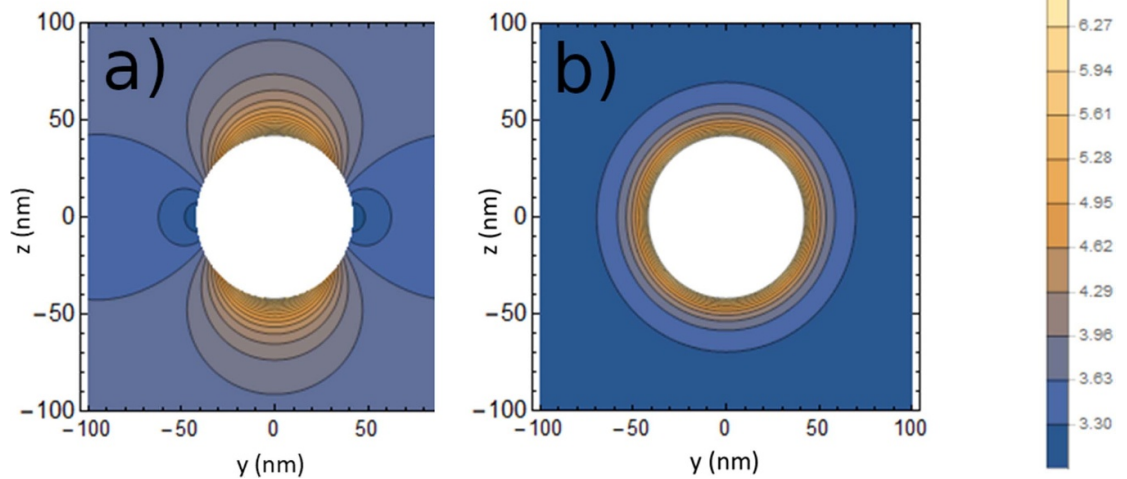


Figure 2. The total near-field intensity normalized by the incident beam intensity in the y - z plane. The light of wavelength 1000 nm is incident on a nanosphere of 40 nm radius with a refractive index of $n = 1.43$. The field inside the nanosphere, shown as the circular white region, is not plotted. (a) Is a plot of the intensity when illuminated by a single field propagating in the x direction and polarized in the z direction. (b) A plot of the intensity when illuminated by three orthogonally propagating fields with orthogonal polarizations.

an atom or nanosphere [31]. When operating close to an atomic resonance the potential is better described by $U_{\text{dip}}(r) = \frac{3\pi c^2}{2\omega_0^3} \frac{\Gamma}{\Delta} I(r)$, where Δ is the detuning of the laser from resonance and Γ is the atomic line width. The potential is inversely proportional to the detuning from an atomic resonance, and such potentials are routinely used to trap cold atoms in free space and more recently in the evanescent fields around a tapered

optical fibre [32]. As the sign of the potential is determined by its detuning with respect to the atomic resonance or resonances, the detuning can be used to produce both repulsive and attractive potentials. The magnitude of the potential can be tuned by controlling the incident light intensity. The maximum potential at any detuning is eventually limited by the resonant excitation of atoms to other internal states or by increased scattering of light, which can lead to recoil heating.

To construct a realistic potential, in addition to the applied optical fields, we must also take into account the strong short-range attractive interactions from the Casimir–Polder (C–P) force and also the charge-induced polarization force between a charged nanosphere and the neutral atom. For charges distributed evenly on the surface, the polarization potential is given by $U = -\frac{1}{(4\pi\epsilon_0)^2} \frac{\alpha_a q^2}{2r^4}$ where q is the total charge on the nanosphere, and α_a is the static polarizability of the atom. For the C–P interaction we consider the non-retarded case where the radius of the sphere is significantly less than the resonance wavelengths [33]. In this case the potential is given by

$$U_{CP} = -\frac{\hbar}{8\pi^2\epsilon_0} \sum_{l=0}^{\infty} (2l+1)(l+1) \times \frac{a^{2l+1}}{r^{2l+4}} \int_0^{\infty} d\zeta \alpha_a(i\zeta) \frac{\epsilon(i\zeta) - 1}{\epsilon(i\zeta) + [(l+1)/l]} \quad (4)$$

where ζ is the angular frequency, α_a is the atomic polarizability, ϵ is the permittivity of the nanosphere and l is an integer [33]. We calculate numerical solutions based on the properties of the silica and the cold atoms. We find that for less than 100 charges on the nanosphere, which is consistent with Paul trapping experiments [28], the C–P force is dominant at all radial distances from the surface of the nanosphere. We therefore only consider the C–P interaction in all subsequent calculations.

Although in principle many laser cooled atoms can be trapped around a nanosphere we consider interactions between metastable helium atoms that can be laser cooled in the 2^3S_1 electronic ground state and a SiO_2 nanosphere of radius $a = 40$ nm. For the metastable helium atoms we need only consider the few allowed transitions to the n^3P states where $n = 2 - 4$ [34].

3. Sympathetic cooling

We first consider sympathetic cooling of a trapped nanosphere by using a single repulsive optical potential created by three intersecting beams to increase the nanosphere collision cross-section so that the nanoparticle can be sympathetically cooled via collisions with surrounding cold atoms. The repulsive field not only increases the cross-section but also prevents atoms from directly colliding with the nanosphere surface, which will remain at 300 K. These types of collision are important to prevent since they would induce recoil heating of the nanosphere by releasing internal energy into the motion of the nanosphere [35]. By using a magic wavelength, where the AC stark shift induced by the potential is the same in the upper and lower electronic states, it is possible to simultaneously laser cool the atoms within the optical potential. This will allow continuous cooling of the atoms around the nanosphere. For metastable helium, a repulsive magic wavelength of 318.611 nm has been previously identified [34].

The full potential for the repulsive optical component $U_R(r)$ and the attractive C–P potential is then given by $U_{TR}(r) = U_R(r) + U_{CP}(r)$, where the optical potential is given by the far off-resonance form $U_R(r) = \frac{1}{2}\alpha_a I_T(r)/\epsilon_0 c$, where $\alpha_a = 1.33 \times 10^{-38} \text{ Cm}^2 \text{ V}^{-1}$ [34] for helium atoms at the magic wavelength. Figure 3 is a plot of the total potential, as a function of radial distance from the centre of the sphere, created by a single beam intensity of $I_0 = 1 \times 10^5 \text{ W cm}^{-2}$. This leads to a well depth of 100 K for the silica nanosphere, which is orders of magnitude smaller than Paul trap confining potential [28]. For small collision energies with E in the $E/k_b = 10 \text{ } \mu\text{K}$ range, typical of ultra-cold atomic gases, only the $1/r$ component needs to be considered.

The scattering of atoms from this potential is then the same form as a repulsive Coulomb potential encountered in classical Rutherford scattering. Without shielding, this type of potential has an infinite total cross-section due to its long range character. However, as the $1/r$ nature of the optical potential results from an interference between incident and scattered fields, and the incidence field has a finite extent, the $1/r$ range will be limited to the incident beam size with a spot size of 20 μm . As we are interested in sympathetic cooling we determine the finite total cross-section, approximating the limited range by using a Yukawa form where $U_Y \approx U_{TR} \exp(-\frac{r}{\mu})$ and where $\mu = 20 \text{ } \mu\text{m}$ [36]. This total cross section in the first Born approximation is given by

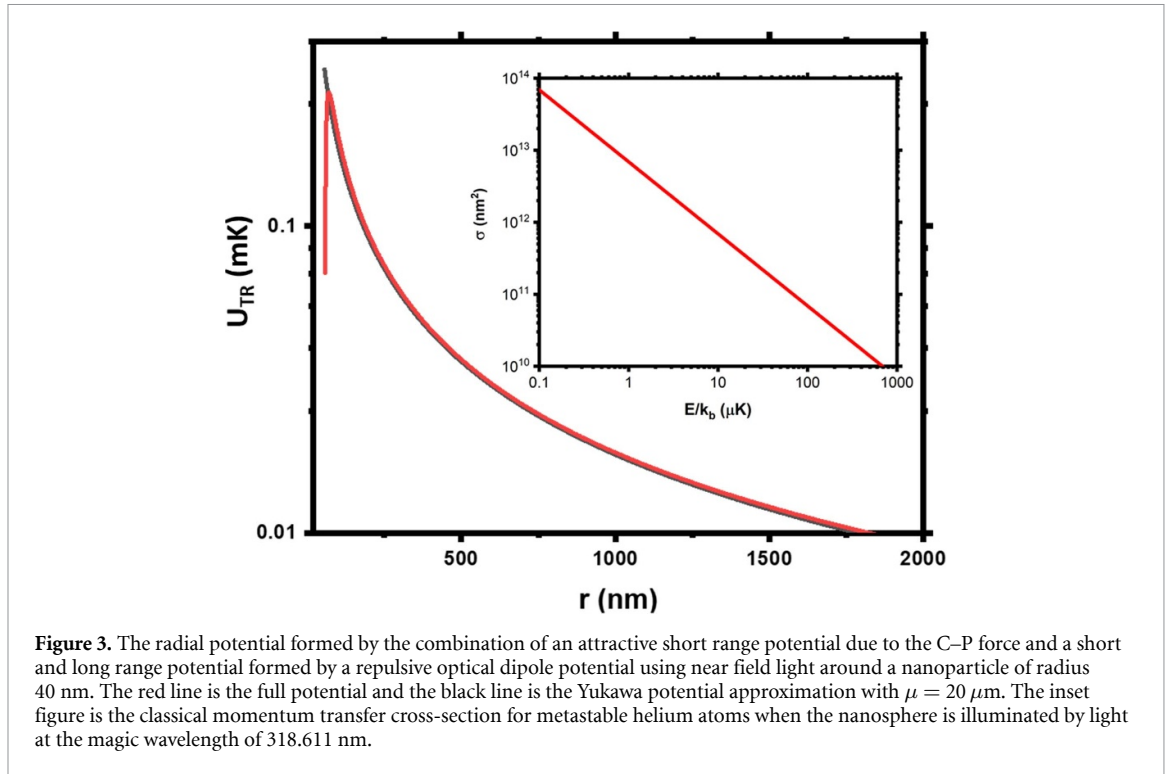


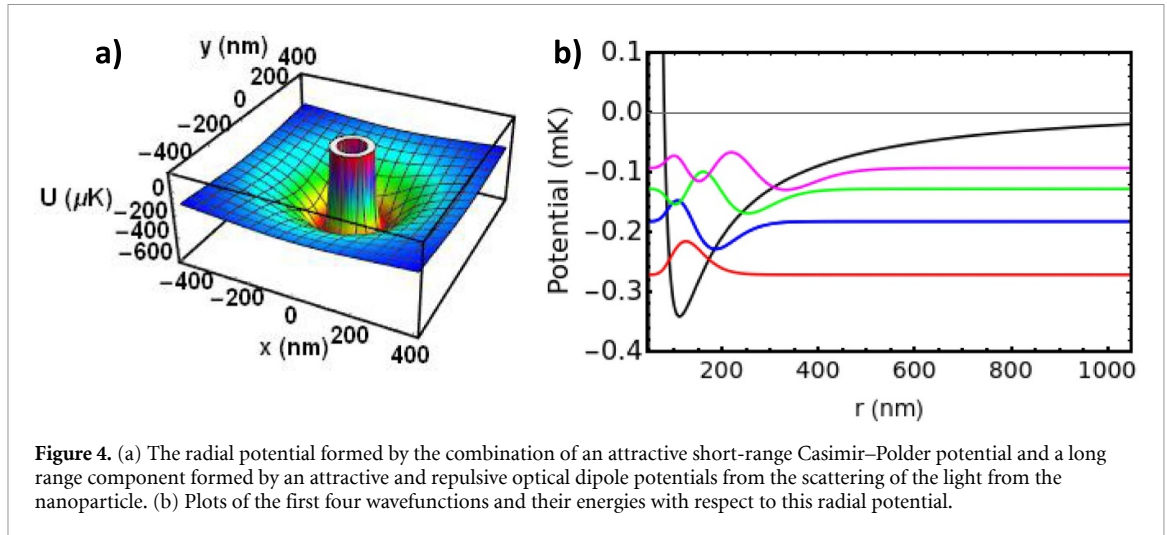
Figure 3. The radial potential formed by the combination of an attractive short range potential due to the C–P force and a short and long range potential formed by a repulsive optical dipole potential using near field light around a nanoparticle of radius 40 nm. The red line is the full potential and the black line is the Yukawa potential approximation with $\mu = 20 \mu\text{m}$. The inset figure is the classical momentum transfer cross-section for metastable helium atoms when the nanosphere is illuminated by light at the magic wavelength of 318.611 nm.

$$\sigma = \frac{16\pi m_a^2 U_T R^2 \mu^4}{\hbar^4 (1 + 4\mu k^2)} \quad (5)$$

which is plotted in the inset in figure 3 as a function of collision energy in units of μK . At a collision energy of $10 \mu\text{K}$, this corresponds to a cross-section of $\sigma = 6.6 \times 10^{11} \text{ nm}^2$, which is more than 8 orders of magnitude larger than the physical cross-section of the 40 nm nanosphere.

The collisional cooling rate of the nanosphere induced by a bath of cold atoms is approximately given by $\gamma_C = \frac{\xi}{\alpha_c} N \langle \sigma(v) \rangle v_{th}$, where the brackets denote the speed averaged cross-section, N is the number density of the gas, $v_{th} = \sqrt{\frac{8k_B}{\pi} \left(\frac{T_a}{m_a} + \frac{T_n}{m_n} \right)}$ is the thermal speed of the gas, and $\alpha_c = 2.7$ is the number of collisions required to thermalize collision partners with equal masses [37]. For unequal masses, as in our case, the cooling rate is reduced by the factor $\xi = \frac{4m_n m_a}{(m_n + m_a)^2}$, where $m_n = 3.2 \times 10^8 \text{ amu}$ is the mass of the nanosphere, and $m_a = 4.0 \text{ amu}$ is the atomic mass. This large mass difference, which usually makes sympathetic cooling inefficient is compensated for by the large cross-section created by the repulsive optical potential. For a silica nanosphere of density $\rho = 2000 \text{ kg m}^{-3}$ with radius 40 nm and a cold atom gas number density of $5 \times 10^{12} \text{ cm}^{-3}$, we determine a cooling/damping rate of $2\pi \times 2.3 \text{ kHz}$ at $T_a = 10 \mu\text{K}$, which can be compared with a damping rate of $2\pi \times 10 \mu\text{Hz}$ for the bare sphere. The ultimate temperature that could be reached will be given by additional technical noise sources, but we estimate an effective temperature from $T_e = (\gamma_C T_C + \gamma_H T_H + \gamma_R T_R) / (\gamma_C + \gamma_H + \gamma_R)$, where γ_C is the the damping rate due to collisions with cold atoms of temperature T_C , γ_H and T_H are the same quantities due to collision with background atoms, while γ_R and T_R are from recoil heating from the light used to form the potential [38]. We do not include the effect of electrical force noise as this depends on supply, trap geometry and charge on the sphere. Assuming a background gas pressure of 10^{-9} mbar of air, we derive a temperature of $14 \mu\text{K}$ for a cold gas temperature of $T_C = 10 \mu\text{K}$ and $2.6 \mu\text{K}$ at $1 \mu\text{K}$. We note that lower background operating pressures in the 10^{-11} mbar range have been reached for cold atom and Paul trap experiments [39]. Trap frequencies up to at least 50 kHz appear feasible for these small nanoparticles levitated in a Paul trap [40] where, at a temperature of $1 \mu\text{K}$ an average phonon occupancy approaching unity could be achieved. In such a scheme ground state cooling may be possible with only small additional feedback cooling.

Although we have considered sympathetic cooling in a Paul trap we point out that such a scheme could also be used in an optical trap formed by three intersecting beams. Here the intensity is orders of magnitude higher than in the Paul trap and the increased heating rate due to photon recoil would not allow cooling to below one Kelvin.



4. Atom-nanosphere bound states

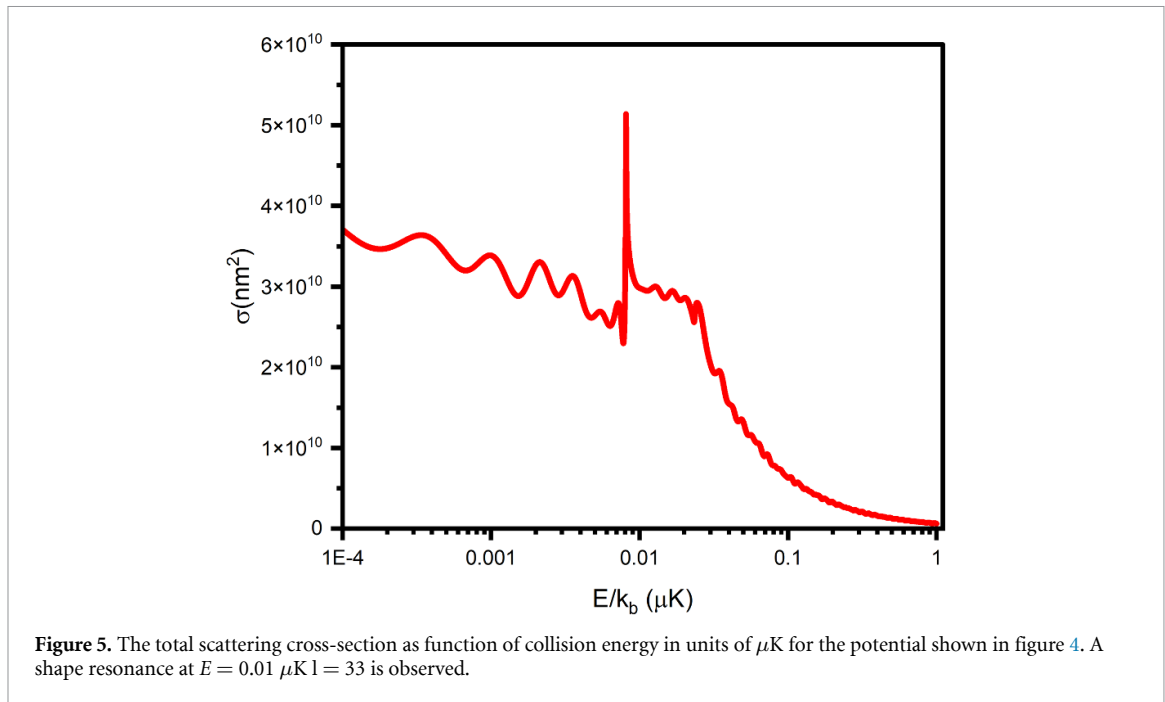
We now explore the creation of a bound atom-nanosphere hybrid system using a combination of both a repulsive and an attractive optical potential given by

$$U_0(r) = U_{CP} + 3(U_R - U_A) + 6 \frac{U_R C_R^2 - U_A C_A^2}{r^6} + 4 \frac{U_R C_R k_R^2 - U_A C_A k_A^2}{r} \quad (6)$$

where U_R and U_A are the maximum repulsive and attractive well depths in the absence of the scattered fields, and U_{CP} is due to the C–P interaction as before. Note that the $1/r^4$ and the $1/r^2$ terms of equation (3) are not significant and are not included here. Initially ignoring the effect of the CP term, which is only dominant at very short range ($r < 50$ nm), the short range ($1/r^6$) optical repulsive term constructed from blue detuned light must exceed the corresponding term for attractive red detuned light. In addition, its maximum value must be significantly greater than the energy of the cold atoms to avoid direct collisions with the surface of the sphere. From equation (5) this condition implies that $U_R C_R^2 > U_A C_A^2$. However, at long range the attractive ($1/r$) potential created by the red detuned field must be larger than the repulsive component so that $U_R C_R k_R^2 < U_A C_A k_A^2$. For a small refractive index variation between the two wavelengths, such that $C_R \approx C_A$, then $k_R^2 < k_A^2$ and the wavelength of light used to construct the repulsive optical potential must therefore be larger than that used for the attractive potential ($\lambda_R^2 > \lambda_A^2$). For a small variation in the refractive index of the nanosphere, we obtain approximate limits of the ratio of the magnitude of the repulsive and attractive potentials given by $1 < \frac{U_R}{U_A} < \frac{\lambda_R^2}{\lambda_A^2}$. Using the $2^3S_1 \rightarrow n^3P$ resonances of metastable helium to enhance the optical well depth, we can choose a blue detuned field (5000 GHz) with respect to the $2^3S_1 - 2^3P$ resonance at 1083 nm to create a repulsive potential, and an attractive potential formed by a field that is red detuned by 100 GHz with respect to the $2^3S_1 - 3^3P$ transition at 389.0 nm. Our choice of wavelength for both potentials limits the ratio of the repulsive to attractive optical potential in the range $1 < U_R/U_A < 7.75$. We explored the properties of this potential for creating bound states for $U_R/U_A = 2.47$ using well depths of $U_R = 2.7$ mK and $U_A = 14.6$ mK. Intensities of approximately 10^5 Wcm² are required, leading to atom trap lifetimes on the order of 10 ms.

Figures 4(a) and (b) are plots of the combined potential, U_0 , which has a well depth of 340 μ K that is sufficient to trap laser-cooled atoms. We calculate the 12 bound states of this potential and the wavefunctions and allowed energies using the Numerov method [41]. These are shown in figure 4 for the first four states. This bound potential is similar to the optical potentials created around tapered optical fibres, and the same techniques can in principle be used to load the atoms into this radially symmetric atom-nanosphere potential [32]. Sideband-resolved cooling has been demonstrated around these tapered optical fibres and could also be used to cool the atoms into the ground state of the optical potential around the nanosphere [42]. As the trapping volume is small (≈ 500 nm³) we expect that collisional blockade will result in only one atom captured in the potential, forming a system that is analogous to a massive diatomic molecule [43].

As the optical potential can be tuned by controlling the relative intensity between the repulsive and attractive fields, resonances could be used to enhance the cross-section and the binding of cold atoms to the nanosphere. Figure 5 is a calculation of the total cross-section as a function collision energy, E , for the potential shown in figure 4. We use the log-derivative method to calculate the wavefunctions for each



potential as a function of collision energy up to 40 partial waves ($l = 40$) [44] which are integrated out to radii of $60 \mu\text{m}$ in order to capture the long range nature of the attractive part of the potential. The wave function phase shifts, δ_l , are determined from their asymptotic solutions and are used to calculate the total cross in the usual way via $\sigma(E) = \frac{4\pi}{k^2} \sum_{l=1}^{20} (2l+1) \sin^2(\delta_l)$, where $k = \sqrt{2m_r E}/\hbar$ and $m_r \approx m_a$ is the reduced mass. The resonance at $E = 0.01 \mu\text{K}$ for $l = 33$ is a shape resonance due to a maximum in the potential at intermediate radii. In the centre-of-mass frame, the collision energy is dominated by the cold atom energy. Observing such low energy resonances will be challenging as they require cold atom energies well below $1 \mu\text{K}$. Here, the necessary energy and energy spread could potentially be prepared using a cold atom collider [45]. Note that the potential and the location of any resonances can be tuned by changing the intensity or the wavelengths of the optical fields that create either the repulsive or attractive potentials. The scattering of cold atoms from these potentials and the measurement of changes to collisional cross section could be used to characterise the C–P potential if the repulsive optical potential was reduced to the point where CP potential is still larger but comparable to the optical potential. This would allow study without ionization of atoms on the nanosphere surface.

5. Experimental implementation

We stress that many laser atomic systems could be used for both sympathetic cooling and for the creation of hybrid nano-particle atom systems including Rubidium and Cesium atoms. We have focused here on laser cooled metastable helium and note that Penning ionisation which could modify the charge on the nanosphere from this species can be strongly suppressed by spin polarizing the atoms. Figure 6 shows a typical setup of such an experiment for creating a magneto optical trap (MOT) for metastable helium [46] which overlaps with the levitated nanoparticle as has been performed for atomic species [47]. For metastable atoms a DC or RF discharge creates an effusive beam of atoms which are decelerated in Zeeman slower to within the capture range of a MOT. This is created by six beams in which three are counterpropagating. The two beams that propagate into and out of the page are not shown. Six circularly beams, at a wavelength of 1083 nm , are used to form the MOT which is surrounded by a quadrupolar magnetic field. The MOT coils are placed outside the final chamber which are not shown for clarity. The Zeeman slower beam counterpropagates to the atomic beam. The Paul trap is placed slightly off-centre from the Zeeman slower beam so that it does not block the beam. The laser beams that create the optical potentials are overlapped with MOT beams and the repulsive component, which has longer range than the CP potential, prevents the atoms from ionising on the surface of the sphere. The DC and AC Paul trap fields prevent charge buildup on the sphere created by any Penning ionisation of the atoms.

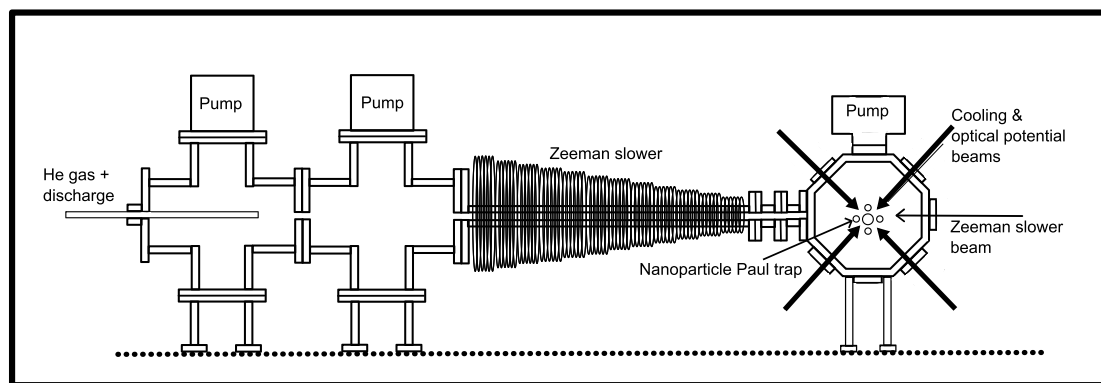


Figure 6. A schematic diagram of laser-cooled metastable helium experiment that incorporates a nanoparticle Paul trap for the creation of the levitated atom-nanosphere hybrid quantum system. An effusive atomic beam of metastable helium atoms created in a gas discharge is decelerated in a Zeeman slower. The atoms are constantly loaded into a magnetic optical trap (MOT). Four of the six MOT cooling beams are shown. The MOT is formed around the levitated sphere within a linear Paul trap. Additional laser beams that are overlapped with the MOT beams form either a single repulsive optical potential used for sympathetic cooling or the combined repulsive and attractive potential to create the atom-nanosphere bound states.

6. Conclusion

We have explored the interactions of a nanosphere with cold metastable helium atoms that form a hybrid atom-nanoparticle quantum system. The general scheme outlined for both sympathetic cooling and the creation of bound states could be also be carried out with most laser-cooled species using different optical wavelengths. We have considered sympathetic cooling in a Paul trap to limit heating via the strong optical fields required for optical trapping. While the micromotion of trapped ions sympathetically cooled by cold atoms limits the achievable final temperature, this effect is strongly suppressed by the more than seven orders of magnitude difference in mass between the nanoparticle mass and the cold [48]. While we have studied near fields around nanoparticles, similar fields created around large macromolecules of similar size particles, such as a virus, could also be cooled. Because many particles are not spherical, a more complicated non-spherical potential will be created. However, sympathetic cooling may still be feasible and, as relatively low intensity fields can be used the optical damage by absorption of light can be minimised when trapped within a Paul trap. We have not treated the effect of the internal mechanical modes of vibration on either the sympathetic cooling or the lifetime of the hybrid system due to motional heating. However, these mechanical modes have frequencies well above either the centre-of-mass motion of the nanosphere or the atom-nanosphere bound state motion and therefore we expect that these will have little effect on the processes studied here. Future work could however additionally explore the sympathetic cooling of the internal temperature of levitated nanospheres and also the rotational motion of non-spherical particles [49]. The sympathetic cooling method studied here for the centre-of-mass motion may offer a very general method for cooling all degrees-of-freedom of a levitated nanoparticle, particularly for multiple co-trapped particles. Finally, the hybrid atom-nanosphere system described here could also be considered as an alternative to Stern–Gerlach Ramsey type interferometry that has been proposed for NV centres [21, 24].

Data availability statement

All data that support the findings of this study are included within the article (and any supplementary files).

Acknowledgment

The authors would like to acknowledge useful discussions with M Toroš, S Bose, A Pontin, A Rahman and G Hetet. The authors acknowledge funding from the EPSRC Grant No. EP/W029626/1 and the H2020-EU.1.2.1 TEQ Project Grant Agreement ID: 766900.

ORCID iD

P F Barker  <https://orcid.org/0000-0001-9669-9853>

References

- [1] Yaakov Y, Fein P G, Zwick P, Kialka F, Pedalino S, Mayor M, Gerlich S and Arndt M 2019 Quantum superposition of molecules beyond 25 kda *Nat. Phys.* **15** 1242
- [2] Romero-Isart O, Juan M L, Quidant R and Ignacio Cirac J 2010 Toward quantum superposition of living organisms *New J. Phys.* **12** 033015
- [3] Romero-Isart O 2011 Quantum superposition of massive objects and collapse models *Phys. Rev. A* **84** 052121
- [4] Bateman J, Nimmrichter S, Hornberger K and Ulbricht H 2014 Near-field interferometry of a free-falling nanoparticle from a point-like source *Nat. Commun.* **5** 4788
- [5] Goldwater D, Paternostro M and Barker P F 2016 Testing wave-function-collapse models using parametric heating of a trapped nanosphere *Phys. Rev. A* **94** 010104
- [6] Anishur Rahman A T M 2019 Large spatial schrödinger cat state using a levitated ferrimagnetic nanoparticle *New J. Phys.* **21** 113011
- [7] Horak P, Hechenblaikner G, Gheri K M, Stecher H and Ritsch H 1997 Cavity-induced atom cooling in the strong coupling regime *Phys. Rev. Lett.* **79** 4974–7
- [8] Koch M, Sames C, Kubanek A, Apel M, Balbach M, Ourjoumtsev A, Pinkse P W H and Rempe G 2010 Feedback cooling of a single neutral atom *Phys. Rev. Lett.* **105** 173003
- [9] Gieseler J, Deutsch B, Quidant R and Novotny L 2012 Subkelvin parametric feedback cooling of a laser-trapped nanoparticle *Phys. Rev. Lett.* **109** 103603
- [10] Kiesel N, Blaser F, Delić U, Grass D, Kaltenbaek R and Aspelmeyer M 2013 Cavity cooling of an optically levitated submicron particle *Proc. Natl Acad. Sci.* **110** 14180–5
- [11] Anishur Rahman A T M and Barker P F 2017 Laser refrigeration, alignment and rotation of levitated Yb^{3+} :YLF nanocrystals *Nat. Photon.* **11** 634
- [12] Delić U, Reisenbauer M, Dare K, Vuletić V, Kiesel N and Aspelmeyer M 2020 Cooling of a levitated nanoparticle to the motional quantum ground state *Science* **367** 892–5
- [13] Tebbenjohanns F, Frimmer M, Jain V, Windey D and Novotny L 2020 Motional sideband asymmetry of a nanoparticle optically levitated in free space *Phys. Rev. Lett.* **124** 013603
- [14] Seberston T, Ju P, Ahn J, Bang J, Tongcang Li and Robicheaux F 2020 Simulation of sympathetic cooling an optically levitated magnetic nanoparticle via coupling to a cold atomic gas *J. Opt. Soc. Am. B* **37** 3714–20
- [15] Son H, Park J J, Ketterle W and Jamison A O 2020 Collisional cooling of ultracold molecules *Nature* **580** 197–200
- [16] Ranjit G, Montoya C and Geraci A A 2015 Cold atoms as a coolant for levitated optomechanical systems *Phys. Rev. A* **91** 013416
- [17] Penny T W, Pontin A and Barker P F 2023 Sympathetic cooling and squeezing of two colevitated nanoparticles *Phys. Rev. Res.* **5** 013070
- [18] Bykov D S, Dania L, Goschin F and Northup T E 2023 3D sympathetic cooling and detection of levitated nanoparticles *Optica* **10** 438–42
- [19] Slezak B R and D’Urso B 2019 A microsphere molecule: the interaction of two charged microspheres in a magneto-gravitational trap *Appl. Phys. Lett.* **114** 06
- [20] Arita Y, Bruce G D, Wright E M, Simpson S H, Zemánek P and Dholakia K 2022 All-optical sub-kelvin sympathetic cooling of a levitated microsphere in vacuum *Optica* **9** 1000–2
- [21] Scala M, Kim M S, Morley G W, Barker P F and Bose S 2013 Matter-wave interferometry of a levitated thermal nano-oscillator induced and probed by a spin *Phys. Rev. Lett.* **111** 180403
- [22] Rahman A T M A, Frangeskou A C, Kim M S, Bose S, Morley G W and Barker P F 2016 Burning and graphitization of optically levitated nanodiamonds in vacuum *Sci. Rep.* **6** 21633
- [23] Delord T, Nicolas L, Bodini M and Hétet G 2017 Diamonds levitating in a paul trap under vacuum: Measurements of laser-induced heating via *nv* center thermometry *Appl. Phys. Lett.* **111** 013101
- [24] Bose S, Mazumdar A, Morley G W, Ulbricht H, Toroš M, Paternostro M, Geraci A A, Barker P F, Kim M S and Milburn G 2017 Spin entanglement witness for quantum gravity *Phys. Rev. Lett.* **119** 240401
- [25] Japha Y and Folman R 2023 Quantum uncertainty limit for stern-gerlach interferometry with massive objects *Phys. Rev. Lett.* **130** 113602
- [26] Delord T, Huillery P, Nicolas L and Hétet G 2020 Spin-cooling of the motion of a trapped diamond *Nature* **580** 56–59
- [27] Toroš M, Bose S and Barker P F 2021 Creating atom-nanoparticle quantum superpositions *Phys. Rev. Res.* **3** 033218
- [28] Bullier N P, Pontin A and Barker P F 2020 Characterisation of a charged particle levitated nano-oscillator *J. Phys. D: Appl. Phys.* **53** 175302
- [29] Novotny L and Hecht B 2006 *Principles of Nano-Optics* (Cambridge University Press)
- [30] Commercial 3D FDTD simulation software 2019 (available at: www.ansys.com/products/optics/fdtd)
- [31] Grimm R, Weidemüller M and Ovchinnikov Y B 2000 Optical dipole traps for neutral atoms *Adv. At. Mol. Opt. Phys.* **42** 95–170
- [32] Vetsch E, Reitz D, Sagué G, Schmidt R, Dawkins S T and Rauschenbeutel A 2010 Optical interface created by laser-cooled atoms trapped in the evanescent field surrounding an optical nanofiber *Phys. Rev. Lett.* **104** 203603
- [33] Hemmerich J L, Bennett R, Reisinger T, Nimmrichter S, Fiedler J, Hahn H, Gleiter H and Yoshi Buhmann S 2016 Impact of casimir-polder interaction on poisson-spot diffraction at a dielectric sphere *Phys. Rev. A* **94** 023621
- [34] Notermans R P M J W, Rengelink R J, van Leeuwen K A H and Vassen W 2014 Magic wavelengths for the $2^3s \rightarrow 2^1s$ transition in helium *Phys. Rev. A* **90** 052508
- [35] Millen J, Deesuwan T, Barker P and Anders J 2014 Nanoscale temperature measurements using non-equilibrium brownian dynamics of a levitated nanosphere *Nat. Nanotechnol.* **11** 425
- [36] Sakurai J J and Napolitano J 2017 *Modern Quantum Mechanics* (Cambridge University Press)
- [37] Ivanov V V, Khramov A, Hansen A H, Dowd W H, Münchow F, Jamison A O and Gupta S 2011 Sympathetic cooling in an optically trapped mixture of alkali and spin-singlet atoms *Phys. Rev. Lett.* **106** 153201
- [38] Jain V, Gieseler J, Moritz C, Dellago C, Quidant R and Novotny L 2016 Direct measurement of photon recoil from a levitated nanoparticle *Phys. Rev. Lett.* **116** 243601
- [39] Dania L, Bykov D S, Goschin F, Teller M and Northup T E 2023 Ultra-high quality factor of a levitated nanomechanical oscillator
- [40] Bell D M, Howder C R, Johnson R C and Anderson S L 2014 Single CdSe/ZnS nanocrystals in an ion trap: charge and mass determination and photophysics evolution with changing mass, charge and temperature *ACS Nano* **8** 2387–98
- [41] Allison A C 1970 The numerical solution of coupled differential equations arising from the schrödinger equation *J. Comput. Phys.* **6** 378–91

- [42] Meng Y, Dureau A, Schneeweiss P and Rauschenbeutel A 2018 Near-ground-state cooling of atoms optically trapped 300 nm away from a hot surface *Phys. Rev. X* **8** 031054
- [43] Schlosser N, Reymond G and Grangier P 2002 Collisional blockade in microscopic optical dipole traps *Phys. Rev. Lett.* **89** 023005
- [44] Johnson B R 1973 The multichannel log-derivative method for scattering calculations *J. Comput. Phys.* **13** 445–9
- [45] Rakonjac A, Deb A B, Hoinka S, Hudson D, Sawyer B J and Kjærgaard N 2012 Laser based accelerator for ultracold atoms *Opt. Lett.* **37** 1085–7
- [46] Bardou F, Emile O, Courty J-M, Westbrook C I and Aspect A 1992 Magneto-optical trapping of metastable helium: collisions in the presence of resonant light *Europhys. Lett.* **20** 681–6
- [47] Eric R H 2016 Sympathetic cooling of molecular ions with ultracold atoms *EPJ Tech. Instrum.* **3** 8
- [48] Cetina M, Grier A T and Vuletić V 2012 Micromotion-induced limit to atom-ion sympathetic cooling in paul traps *Phys. Rev. Lett.* **109** 253201
- [49] Pontin A, Fu H, Toroš M, Monteiro T S and Barker P F 2023 Simultaneous cavity cooling of all six degrees of freedom of a levitated nanoparticle *Nat. Phys.* **19** 1003–8